Hindawi Publishing Corporation
Mathematical Problems in Engineering
Volume 2014, Article ID 710512, 11 pages
http://dx.doi.org/10.1155/2014/710512

Research Article

Fixed-Order Robust H_∞ Estimator Design for Side-Slip Angle of Vehicle

Akın Delibaşı

Department of Control and Automation Engineering, Yıldız Technical University, Esenler, 34220 Istanbul, Turkey

Correspondence should be addressed to Akın Delibaşı; adelibas@yildiz.edu.tr

Received 30 May 2014; Revised 3 October 2014; Accepted 19 October 2014; Published 9 November 2014

Academic Editor: Driss Mehdi

We present a novel linear observer with an extension dealing with polytopic uncertainties in a vehicle dynamic system to identify the side-slip angle. The performance optimization issue is addressed by the minimization of H_∞ norm of the system considering the estimation error as an output and the steer angle as an input. Contrary to the standard robust optimal design approaches, we use a convex inner approximation technique to reduce the order of the observer and this enables us to derive suboptimal, fixed-order, and efficiently practicable estimators. Moreover, the numerical examples performed on two-track nonlinear model of the system are provided to illustrate the impacts of design parameters on the optimization results and the efficiency of the technique.

1. Introduction

Active vehicle safety systems such as rollover prevention, lane departure avoidance, and yaw stability control require real time information about the side-slip angle of vehicle in order to function accurately during the run-time [1, 2]. Particularly, the control of yaw rate is felt short to prevent drift-out in a low-friction track. In addition to yaw rate control in a low-friction track, the skid prevention system should be supported with a side-slip angle controller [3, 4]. Therefore, the vehicle stability control unit requires the measurement of the yaw rate and the side-slip angle of vehicle. Mainly, two types of sensors such as optical and GPS based are used to measure the side-slip angle directly [5]. The accuracy of GPS based sensors hinges on the weather conditions and they may not provide reliable data especially in bad weather conditions. Although the optical ones can provide the accurate measurements, both types of sensors are too expensive to use in commercially competitive products [6]. Hence, it needs to be estimated by virtual sensors [7].

In the literature, the topic is still hot and deserves interest due to the importance of issue in human life. Two main methods are mostly used in the previous studies for the estimation of side-slip angle. These are model based and kinematics-based methods [1, 2]. Even though the kinematic-based ones have significant advantages such as easy implementation and robustness against uncertain parameters of the vehicle model, they are sensitive to sensor errors. In [5, 8], they describe a methodology for estimating vehicle slip angle based on a nonlinear model while Venhovens and Naab represent a stochastic state estimator with Kalman filter using a linear model [9]. Besides, Kiencke and Daib compare both linear and nonlinear model based estimators by using a high-order nonlinear model [10]. In [11], they provide a nonlinear model based estimator which has a comparatively acceptable computational cost. According to the outcomes of these studies, there is a clear trade-off between computational cost and accuracy. The nonlinear model based estimators have considerable amount of accuracy but high computational costs when compared to the linear model based ones. Thus, the accuracy improvement is a significant issue for the linear model based estimators.

However, the efficiency of the model based estimators hinges on the knowledge of model parameters. It is well known that the vehicle systems have lots of physical parameters, which are unknown or difficult to estimate. In addition to this problem, some of the model parameters such as velocity and road friction coefficients vary during vehicle maneuvers. In order to cope with these difficulties, the adaptive estimation strategies are proposed in [12–15]. The drawback of these approaches is again their high computational costs.

Therefore, they may not be efficiently implemented on embedded systems. The vehicle models also have uncertainties as well as varying model parameters. Hence, they should be considered in design processes to obtain a robust estimate of side-slip angle. In the previous studies, they increase the level of robustness either by adding extra measurements such as lateral tire forces or using six degree of freedom inertial sensor cluster [16, 17]. By the help of these extra measurements, their approaches do not depend on vehicle or friction model anymore. Therefore, their estimators are robust against parametric uncertainties of the model.

To the best of the author's knowledge, there is no such robust estimator design considering parametric uncertainties especially on the vehicle model in the literature although there are several studies for the robust estimators such as algebraic Riccatti equation based approach [18], Krein space estimation approach [19], and LMI based approach [20, 21]; one can refer to [22] for a survey on the topic. The standard design of robust optimal estimator provides an estimator with the same order of the generalised system derived from a plant and weighted functions, which are mostly at very high degrees [23]. However, a high order estimator may not be efficiently used in commercially competitive products such as four-wheel standard vehicles due to their high costs.

One of the main purposes of this study is to represent a low order estimator. The main obstruction in the development of fixed-order or structured estimators is that the solution set for the coefficients of characteristic polynomial is generally nonconvex. Yet there is no polynomial-time solver for nonconvex solution sets. In order to deal with this problem, inner [24] and outer [25] convex approximation techniques are used. Lasserre's hierarchy of LMI relaxations can be adopted to find the outer approximated region for nonconvex sets which are semidefinite representable [26]. The main difference between these two techniques is that the outer one provides the necessary condition and the inner one provides the sufficient condition. Hence, we use inner approximation to assure the solution located in the exact region. The least conservative inner approximation technique uses Linear Matrix Inequality (LMI) regions by the help of the strict positive realness lemma [24]. According to Henrion et al., the gap between approximated and nonconvex regions extremely depends on the location of the central polynomial [24]. Some of the geometrical constraints are used to solve the H_∞ norm minimization problem via the inner approximation technique [27]. This idea is extended by Yang et al. using the information of bound on the norm of model uncertainties. Thus, this technique eliminates the geometric constraints on the definition of problem [28].

In this paper, we propose a design technique to obtain a robust fixed-order H_∞ estimator for side-slip angle. The estimator ensures suboptimal H_∞ norm level of the system between steer angle and estimation error by considering the uncertainties on velocity and cornering stiffness.

The notation to be used in the paper is fairly standard. $\mathbb{R}$ stands for the set of real numbers and $\mathbb{Z}_+$ symbolizes the set of positive integers. The identity matrices are denoted by I. $X \geq 0$ ($X > 0$) denotes that X is a positive semidefinite (positive definite). The asterisk symbol ($*$) denotes complex conjugate. b_i and $b_{i,j}$ denote the entry of vector b and matrix B, respectively. $A \subset B$ means that A is a subset of B. The overdot denotes the derivative with respect to time. Finally, the notation $\star$ denotes off diagonal entries of a symmetric matrix.

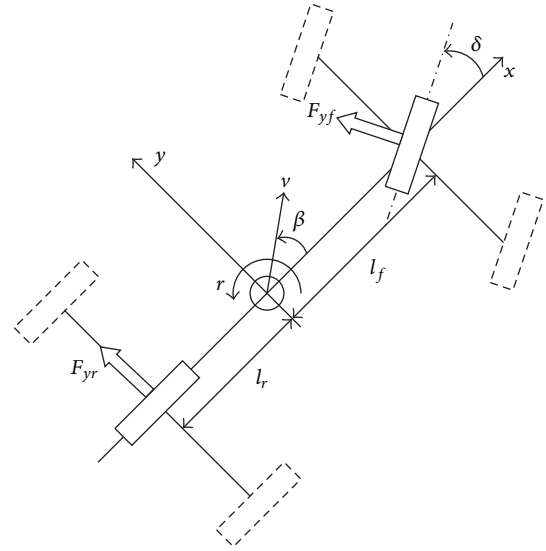

Figure 1: Single track model.

The rest of the paper is organized as follows. The vehicle model, which is considered in the problem, is given in Section 2. In Section 3, the convex inner approximation is presented. The extension of the proposed method to H_∞ performance is studied in Section 4. The numerical example is presented in Section 5 to demonstrate the effectiveness of the fixed-order estimator. The paper is concluded with remarks and future works in the final section.

2. The Vehicle Model

Lateral motion dynamics of a vehicle have been studied for more than a half-century. A convenient vehicle model for low g cornering maneuver is a single track model, also known as bicycle model, shown in Figure 1. This model has essential features of a vehicle's lateral and yaw rate dynamics [29].

The main assumption of the model is the combination of two front and two rear tires as one front and one rear tire, respectively. Neglecting roll, pitch, and bounce dynamics, one can derive the equation of motion of the single track model as follows:

$$\begin{aligned} M\left(\dot{v}_y + v_x r\right) &= F_{yf} + F_{yr}, \\ J_z \dot{r} &= l_f F_{yf} - l_r F_{yr}, \end{aligned} \tag{1}$$

where M, v, r, l_f, and l_r represent total mass, velocity, yaw rate ($r \equiv \dot{\psi}$), distance from center of gravity to front, and rear wheel, respectively. F_{yf} (F_{yr}) denotes y-axis component of the force vector for front tire (rear tire). Here, J_z denotes the total inertia of vehicle on the z-axis.

Assuming that the tire model is linear, we can accept $F_{yf} = C_f \alpha_f$, $F_{yr} = C_r \alpha_r$ and the side-slip angle

$\beta = \tan(v_y/v_x) \approx v_y/v_x$ where α stands for the tire lateral slip angle. Then, the classical linear bicycle model can be obtained as

$$\begin{aligned}\dot{\beta} = & -\frac{1}{Mv}\left(C_f + C_r\right)\beta \\ & + \left[-1 + \frac{1}{Mv^2}\left(-l_f C_f + l_r C_r\right)\right] r + \frac{1}{Mv} C_f \delta, \\ \dot{r} = & \frac{1}{J_z}\left(-l_f C_f + l_r C_r\right)\beta \\ & - \frac{1}{J_z v}\left(l_f^2 C_f + l_r^2 C_r\right) r + \frac{l_f}{J_z} C_f \delta,\end{aligned} \tag{2}$$

where δ represents the steering angle. Then, one can write the transfer functions of the system from the steer angle, δ, to the side-slip angle, β, as

$$\begin{aligned}p_1(s) = & \frac{b_1(s)}{a(s)} \\ = & \left(J_z v^3 C_f s + \left(C_f l_f^2 v^2 - C_f l_f^2 - l_f m v^2 \right.\right. \\ & \left.\left. + \; l_f C_r l_r - C_r l_r^2 v^2\right) C_f\right) \\ & \times \left(m v^2 J_z s^2 \right. \\ & + \left[m v\left(C_f l_f^2 - C_r l_r^2\right) + J_z v\left(C_f + C_r\right)\right] s - 2 C_r^2 l_r^2 \\ & \left. + \left[\left(l_f^2 - l_r^2 + 2 l_f l_r\right) C_f + l_r m v^2\right] C_r - C_f C_r l_r^2\right)^{-1},\end{aligned} \tag{3}$$

and from the steer angle, δ, to the yaw rate, $\dot{\psi}$, as

$$\begin{aligned}p_2(s) = & \frac{b_2(s)}{a(s)} \\ = & \left(m v^2 C_f l_f s \right. \\ & \left. - v C_f\left(C_f l_f v^2 - C_r l_f - C_r l_r v^2 - C_f l_f\right)\right) \\ & \times \left(m v^2 J_z s^2 \right. \\ & + \left[m v\left(C_f l_f^2 - C_r l_r^2\right) + J_z v\left(C_f + C_r\right)\right] s - 2 C_r^2 l_r^2 \\ & \left. + \left[\left(l_f^2 - l_r^2 + 2 l_f l_r\right) C_f + l_r m v^2\right] C_r - C_f C_r l_r^2\right)^{-1}.\end{aligned} \tag{4}$$

Since cornering stiffness parameters and velocity appear multiaffinely, we may deal with the uncertainties associated with these parameters by introducing $p_1(s,\lambda)$ and $p_2(s,\lambda)$ polynomials representing the systems inside the polytope vertices where λ denotes the coordinate of the system in polytope.

As mentioned above, the goal of our estimator is to reduce H_∞ norm of the system, which is defined between the steer angle and the estimator error ($z = \beta - \widehat{\beta}$), through a fixed-order estimator. β and $\widehat{\beta}$ stand for the actual side-slip angle and the suboptimally estimated side-slip angle, respectively.

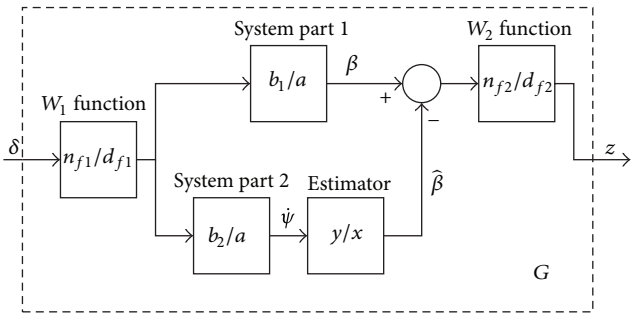

Figure 2: System between performance output and steer angle input.

To make the design as close as possible to the driver steering command in real world, we assume that the steering angle may not vary faster than 1 Hz. Therefore, a second order low pass filter in the form of

$$W_1(s) = \frac{n_{f1}(s)}{d_{f1}(s)} = \frac{39.4784}{s^2 + 8.8858 s + 39.4784} \tag{5}$$

is placed just after the steering angle signal in order to increase the realism and the efficiency of the design. Moreover, another weighting function to reduce the tracking error is specified as follows:

$$W_2(s) = \frac{n_{f2}(s)}{d_{f2}(s)} = \frac{0.01}{s + 0.01}, \tag{6}$$

which is used after the output error signal. In Figure 2, we may see the scheme of the nominal system from the steer angle δ to the performance output z. Hence the transfer function from δ to z is obtained as

$$\begin{aligned}G(s,\lambda) = & \left(n_{f1}(s)\, b_1(s,\lambda)\, x(s)\, n_{f2}(s) \right. \\ & \left. - n_{f1}(s)\, b_2(s,\lambda)\, y(s)\, n_{f2}(s)\right) \\ & \times \left(d_{f1}(s)\, a(s,\lambda)\, x(s)\, d_{f2}(s)\right)^{-1},\end{aligned} \tag{7}$$

where $y(s)$ and $x(s)$ denote the numerator and denominator polynomials of the estimator, respectively.

3. Convex Inner Approximation

In this section, we briefly recall the convex inner approximation technique proposed in [24] which is used to find the fixed-order $y(s)/x(s)$ estimator. The proposed approximated region is represented by an LMI using the theory of positive polynomials. The core idea of this approach is based on the strict positive realness (SPRness) of the rational function.

Let us define a region in the complex plane in the form of

$$\mathscr{D} = \left\{ s \in \mathbb{C} : \begin{bmatrix}1\\ s\end{bmatrix}^* \underbrace{\begin{bmatrix}\delta_{11} & \delta_{12}\\ \delta_{12}^* & \delta_{22}\end{bmatrix}}_{\Delta} \begin{bmatrix}1\\ s\end{bmatrix} < 0 \right\}. \tag{8}$$

Standard choices for Δ are the left half-plane ($\delta_{11} = 0, \delta_{12} = 1, \delta_{22} = 0$) for the continuous polynomial and the unit disk ($\delta_{11} = -1, \delta_{12} = 0, \delta_{22} = 1$) for the discrete polynomial. Let

$$\partial\mathscr{D} = \left\{s \in \mathbb{C} : \delta_{11} + \delta_{12}s + \delta_{12}^{*}s^{*} + \delta_{22}ss^{*} = 0\right\} \quad (9)$$

be the one-dimensional boundary of the region $\mathscr{D}$. A polynomial is called $\mathscr{D}$-stable, when its roots belong to $\mathscr{D}$. Similarly, a rational function is $\mathscr{D}$-strict positive real ($\mathscr{D}$-SPR) if and only if its real part is positive when evaluated along $\partial\mathscr{D}$. As $\mathscr{D}$ stability is a less conservative convex condition than quadratic stability [30], we choose to use $\mathscr{D}$ stability condition in this study.

Let us now consider two polynomials, $c(s) = c_0 + c_1 s + \cdots + c_n s^n$ and $d(s) = d_0 + d_1 s + \cdots + d_n s^n$ of degree n, with real coefficient vectors

$$c = \begin{bmatrix} c_0 & c_1 & \cdots & c_n \end{bmatrix}, \qquad d = \begin{bmatrix} d_0 & d_1 & \cdots & d_n \end{bmatrix}. \quad (10)$$

$c(s)$ is called central polynomial and it is the main design parameter. Then Hermitian matrix $P(c)$ is constructed as

$$P(c) = d^{*}c + c^{*}d - 2\epsilon_1 c^{*}c, \quad (11)$$

where ϵ_1 denotes a small positive scalar.

After these definitions, we may use the key idea ($\mathscr{D}$-SPRness of the rational function) to describe the LMI region.

Corollary 1. *For a given $\mathscr{D}$-stable polynomial $c(s)$, polynomial $d(s)$ is also $\mathscr{D}$-stable if the rational function $d(s)/c(s)$ is $\mathscr{D}$-SPR.*

In the sequel, we may formulate $\mathscr{D}$-SPRness of $d(s)/c(s)$ via polynomial positivity. The SPRness condition is characterized by

$$\begin{aligned} \operatorname{Re}\frac{d(s)}{c(s)} &= \frac{1}{2}\left(\frac{d^{*}(s)}{c^{*}(s)} + \frac{d(s)}{c(s)}\right) \\ &= \frac{1}{2}\left(\frac{d^{*}(s)\,c(s) + c^{*}(s)\,d(s)}{c^{*}(s)\,c(s)}\right) \geq \epsilon_1. \end{aligned} \quad (12)$$

Owing to this formulation, one can define the positivity condition as follows:

$$p(s) = d^{*}(s)\,c(s) + c^{*}(s)\,d(s) - 2\epsilon_1 c^{*}(s)\,c(s) \succeq 0 \quad (13)$$

for all $s \in \partial\mathscr{D}$.

In addition to these aforementioned definitions, we will show the asymptotic convergence of the estimation error of side-slip angle to zero through the well-known Lyapunov stability theorem. In order to do so, we choose a fictitious state vector to be as

$$\xi(t) = \left[\nu(t) \quad \frac{d^n z(t)}{dt^n}\right]^{*}, \quad (14)$$

where $\nu(t)$ is defined as

$$\nu(t) = \left[\, z(t) \quad \frac{dz(t)}{dt} \quad \cdots \quad \frac{d^{n-1}z(t)}{dt^{n-1}} \,\right]^{*}, \quad (15)$$

and let

$$\Pi = \begin{bmatrix} \Pi_1 \\ --- \\ \Pi_2 \end{bmatrix} = \begin{bmatrix} 1 & & & 0 \\ & \ddots & & \vdots \\ & & 1 & 0 \\ - & - & - & - \\ 0 & 1 & & \\ \vdots & & \ddots & \\ 0 & & & 1 \end{bmatrix} \quad (16)$$

be the linear mapping matrix of size $2n \times (n+1)$. Now one can reformulate the state vector definition as $\nu(t) = \Pi_1 \xi(t)$ and $\dot{\nu}(t) = \Pi_2 \xi(t)$. The projected stability matrix can be defined as

$$\Delta(Q) = \Pi^{*}(\Delta \otimes Q)\,\Pi, \quad (17)$$

where $\otimes$ is the Kronecker product.

Lemma 2. *Given a $\mathscr{D}$-stable polynomial $c(s)$ of degree n, polynomial $d(s)$ is also $\mathscr{D}$-stable if there exists a matrix Q of size n solving the LMI*

$$P(c) - \Delta(Q) \succeq 0, \quad Q = Q^{*}. \quad (18)$$

Proof. A proof based on polynomials positivity is described in [24]. Here we represent the asymptotic stability of the system using Lyapunov function in order to guarantee the performance for the time-varying parameters [31]. One can write the quadratic Lyapunov function as

$$V(t) = \xi^{*}(t)\,\Pi_1^{*} Q \Pi_1 \xi(t) \quad (19)$$

since the Lyapunov function is defined by $V(t) = \nu^{*}(t)Q\nu(t)$. The time-derivative of the Lyapunov function is $\dot{V}(t) = -\xi^{*}(t)\Delta(Q)\xi(t)$ [32]. Then, the conditions

$$\begin{aligned} \xi^{*}(t)\,Q\xi(t) > 0, \\ -\xi^{*}(t)\,\Delta(Q)\,\xi(t) < 0 \end{aligned} \quad (20)$$

guarantee the Lyapunov stability along the system trajectory $d\xi(t) = 0$. The proof can be concluded by applying Finsler's lemma to (20). The equivalent statements of Finsler's lemma state that there exists a vector c which ensures (18) and $Q > 0$. The condition $Q > 0$ can be omitted since $c(s)$ is stable. □

Remark 3. Since ϵ_1 needs to be any positive scalar, we may set a very low value to it. Hence, $-2\epsilon_1 c^{*}c$ term can be negligible in (11).

To the best of our knowledge, this technique is the least conservative inner approximation in the literature.

4. H_∞ Performance

Most of the previous studies on H_∞ performance are based on the state space representation. Kučera's [33] and Kwakernaak's [34] works are some of the rare analyses on this performance through polynomial representation. The salient advantage

of this representation is that it provides an opportunity to design a fixed-order estimator which guarantees an H_∞ performance.

Assume that the polynomial $d(s)$ is affected by an additive norm-bounded uncertainty in the form of

$$d_\zeta(s) = d(s) + \zeta n(s), \quad |\zeta| \le \gamma^{-1}, \tag{21}$$

where ζ is a real-valued scalar of unstructured uncertainty. According to the small-gain theorem, robust stability of polynomial is equivalent to the H_∞ performance constraint

$$\left\| \frac{n(s)}{d(s)} \right\|_\infty < \gamma \tag{22}$$

on the transfer function [23].

Theorem 4. *For a given $\mathcal{D}$-stable polynomial $c(s)$, the transfer function $n(s)/d(s)$ is also $\mathcal{D}$-stable and ensures the H_∞ performance constraint if there exist a symmetric matrix Q and a scalar ϵ_2 such that*

$$\begin{bmatrix} c^*d + d^*c - \epsilon_2 c^*c - \Pi^*(\Delta \otimes Q)\Pi & n^* \\ n & \epsilon_2\gamma^2 \end{bmatrix} \succeq 0. \tag{23}$$

The proof of this theorem follows from the application of Lemma 2 to uncertain polynomial $d_\zeta(s)$ and then it yields the uncertain LMI

$$c^*(d + \zeta n) + (d^* + n^*\zeta)c - \Delta(Q) \succeq 0 \tag{24}$$

which is equivalent to the following quadratic inequality:

$$\eta^* \left(c^*(d + \zeta n) + (d^* + n^*\zeta)c - \Delta(Q) \right) \eta \ge 0, \tag{25}$$

for an arbitrary vector η. Defining $r := \zeta c\eta$, one can rewrite (25) as follows:

$$\begin{bmatrix} \eta \\ r \end{bmatrix}^* \begin{bmatrix} c^*d + d^*c - \Delta(Q) & n^* \\ n & 0 \end{bmatrix} \begin{bmatrix} \eta \\ r \end{bmatrix} \succeq 0. \tag{26}$$

For the rest of the proof related with the performance criteria, we may rewrite $|\zeta| \le \gamma^{-1}$ bound over the uncertainty as $\gamma^{-2} - \zeta^2 \ge 0$ or equivalently in the form of quadratic inequality

$$\eta^* c^* c\eta - \gamma^2 r^* r \ge 0. \tag{27}$$

Then, adopting the S-procedure on (26) and (27), it is straightforward to obtain the LMI introduced in (23).

We can extend Theorem 4 to the case of uncertain system $n(s,\lambda)/d(s,\lambda)$, discussed in the modeling section, which is located in the polytope with vertices $(n^i(s)/d^i(s))$ $(i = 1, 2, \ldots, N)$, where $n^i(s) = n_0^i + n_1^i s + \cdots + n_m^i s^m$ and $d^i(s) = d_0^i + d_1^i s + \cdots + d_m^i s^m$ for $i = 1, 2, \ldots, N$. From the structure of our estimator design, shown in Figure 2, the numerator and denominator of $G(s,\lambda)$ are related with the estimator's numerator and denominator represented by $y(s)$ and $x(s)$ polynomials. Therefore, we may define the coefficient vectors $n^i(x,y)$ and $d^i(x,y)$ for the vertices of polytope.

Lemma 5. *Given a stable $c(s)$ and $\gamma > 0$, the uncertain polynomial $d(s,\lambda)$ in the vertices of $n^i(s)$ and $d^i(s)$ ensures SPRness of $d(s,\lambda)c^{-1}(s)$ and satisfies the H_∞ performance constraint if and only if there exist matrices $Q^i = Q^{i*}$, vectors x, y, and scalars ϵ_2^i, such that the inequalities*

$$\begin{bmatrix} c^*d^i(x,y) + d^i(x,y)^* c - \epsilon_2^i c^*c - \Pi^*\left(\Delta \otimes Q^i\right)\Pi & n^i(x,y)^* \\ n^i(x,y) & \epsilon_2^i\gamma^2 \end{bmatrix} \succeq 0, \tag{28}$$

are satisfied for all $i = 1, 2, \ldots, N$.

5. Numerical Results

This section investigates the effectiveness of the proposed estimator. The single-track linear model is used to design estimators. In order to make a realistic investigation, we consider a two-track nonlinear model to test the proposed estimators under some standard lateral dynamics maneuvers. Fundamentally, the two-track nonlinear model is considered as a complete vehicle model for lateral and longitudinal dynamics which is well defined in Kiencke's book (Section 8.4 the complete vehicle model, page 341) [35]. Since we focus on the lateral movements, we may neglect the longitudinal forces and define velocity as an input of the system. Due to the page limitation, the detailed representation of the model is omitted. The parameters used for the vehicle model are given as $M = 1500\,\text{kg}$, $l_f = 1.4\,\text{m}$, $l_r = 1.7\,\text{m}$, $b_r = b_f = 1.6\,\text{m}$ (distance between wheels), $k_G = 1.3\,\text{m}$, and $J_z = Mk_G^2$, where k_G is turning radius. The cornering stiffness value hinges on several parameters such as the type of the tire, the inflating pressure, and the vertical load. During the maneuver, the velocity is not certain. Therefore, we consider them as uncertainty parameters and assume that C_{r_j}, C_{f_j}, and v values vary in [550 N/deg 650 N/deg], [590 N/deg 610 N/deg], and [20 km/h 40 km/h] intervals for all $j = \{r, l\}$, respectively. Here, C_{r_r} and C_{r_l} denote cornering stiffness parameters for rear right and left tires. The front tires' parameters are also defined by the same way.

The uncertain parameters C_r, C_f, and v appear multiaffinely in single-track model and they can be overbounded in design process. Therefore, the coefficients of $b_1(s,\lambda)$, $b_2(s,\lambda)$, and $a(s,\lambda)$ polynomials vary in 6 distinct intervals, producing a polytope of system with $N = 2^6 = 64$ vertices. The polytopic system can be defined as follows:

$$\begin{aligned} \frac{b_1(s)}{a(s)} &= \frac{\overbrace{[2.1869, 4.5221]}^{\text{interval 1}}\, s + \overbrace{[-0.4460, -0.3923]}^{\text{interval 2}}}{s^2 + \underbrace{[0.0487, 0.1111]}_{\text{interval 3}} s + \underbrace{[0.0280, 0.1080]}_{\text{interval 4}}}, \\ \frac{b_2(s)}{a(s)} &= \frac{\overbrace{[0.3258, 0.3369]}^{\text{interval 5}}\, s + \overbrace{[0.1191, 0.5056]}^{\text{interval 6}}}{s^2 + \underbrace{[0.0487, 0.1111]}_{\text{interval 3}} s + \underbrace{[0.0280, 0.1080]}_{\text{interval 4}}}. \end{aligned} \tag{29}$$

As we noted in the introduction that the main motivation of this work is to find fixed-order estimators which provide

similar performance as full-order one. The full-order estimator can be designed by using the theory in [36] which is well known and easy to obtain through "hinfsyn" function in MATLAb. In order to present the conservatism and the achievements of fixed-order estimator, we design the full-order H_∞ estimator,

$$\begin{aligned}\frac{y(s)}{x(s)} = &\left(29.1527s^4 + 1668.0568s^3\right.\\ &+ 53575.7938s^2 + 761774.0604s\\ &\left.- 8190984.7539\right)\\ &\times \left(s^5 + 174.3576s^4 + 12000.3376s^3\right.\\ &+ 461263.0713s^2 + 8421075.3411s\\ &\left.+ 889136.54492\right)^{-1}\end{aligned} \tag{30}$$

which ensures $\gamma = 2$. Although the full-order one is easy to design and it provides the optimal result, it may be hard to implement on a real system. In addition to this, the reliability level of estimator is inversely proportional to the degree of full-order estimator. Therefore, low-order estimators or controllers, especially first or second order, are preferred. Moreover, it is easier to tune low-order estimators compared to full-order ones.

Our goal is to find the first degree estimator $y(s)/x(s)$ which ensures the minimum achievable H_∞ norm of the transfer function (7) for all possible values of the uncertain parameter λ. During the simulation studies, $\mathcal{D}$-region is considered as the open left-half plane, so $\delta_{11} = \delta_{22} = 0$, $\delta_{12} = 1$, and $\epsilon_2 = 1$.

In order to define a convex problem, we should assign the coefficients of central polynomial in the problem (28). The basic strategy is that zeros of central polynomial are chosen around the nominal system's poles which are obtained by using unity gain as the estimator and then move some of the slow poles to improve the dynamic response. In order to do so, we need to find the poles of this system which are located at $(-4.4429 \pm i4.4429, -0.1210 \pm i0.2598, -0.01)$ and then we may add one more pole for first order estimator and move the slow poles slightly to the left to improve the dynamic response. Since the desired estimator is degree one, we may choose the roots of central polynomial as $(-4.4429 \pm i4.4429, -0.1210 \pm i0.2598, -0.1 \pm i0.01)$. According to this strategy, the central polynomial is

$$\begin{aligned}c(s) = &\, s^6 + 9.3278s^5 + 43.5467s^4\\ &+ 18.7172s^3 + 5.7164s^2 + 0.7516s + 0.0327.\end{aligned} \tag{31}$$

Finally, we obtain the first degree robust estimator,

$$\frac{y(s)}{x(s)} = \frac{1.8762s - 6.6020}{5.8268s + 0.8428}, \tag{32}$$

by solving the convex optimization problem: minimize γ subject to LMI problem (28) using YALMIP [37] with SeDuMi [38] solver. The estimator yields $\gamma = 3.7817$. One can observe in Figure 3 that the performance criteria are ensured for all 64 vertices by the proposed estimator.

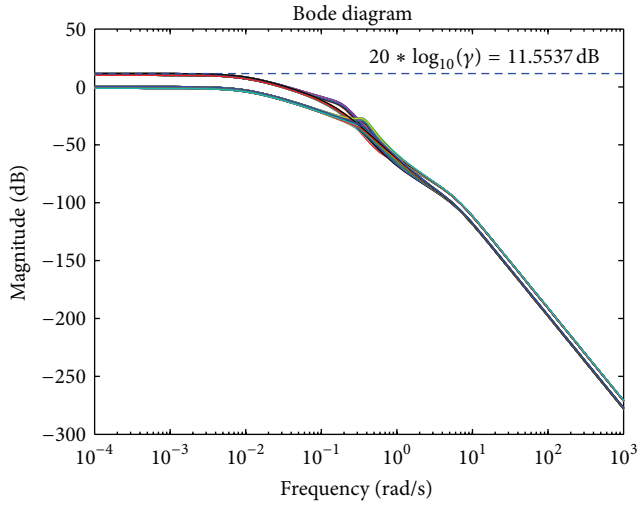

Figure 3: Bode plot of the system for all vertices.

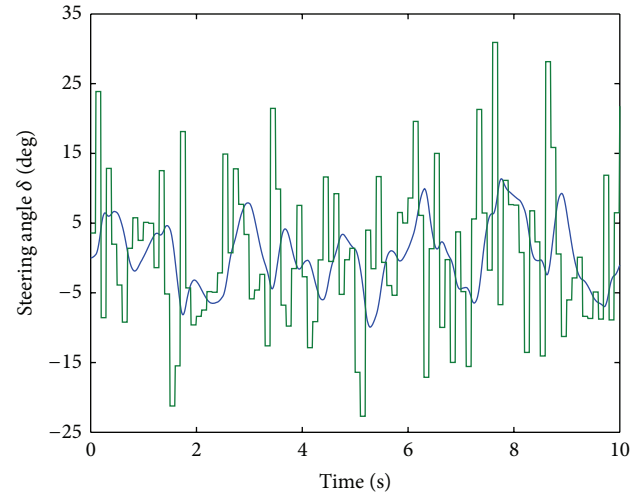

Figure 4: Band limited white noise signal used for the simulation of the steer angle input (green line) and filtered steer angle input (blue line).

In order to emphasize the robustness of the proposed estimator, the system is driven by a steering angle (δ). The realistic steer angle signal is produced by filtering the output of the "Band-Limited White Noise" (BLWN) block in Matlab-Simulink with the filter W_1 where BLWN uses 10 for the noise power value and 0.1s for the sample time value. One can see in Figure 4 that the output of W_1 filter, colored in blue, produces a realistic steering angle signal for the simulation. The velocity (v) and the cornering stiffness parameters (C_{r_r}, C_{r_l}, C_{f_r}, and C_{f_l}) vary in the intervals shown in Figure 5.

The output of the full-order and proposed estimator are presented in Figure 6. In some applications, the designer may request a better dynamic response which can be obtained by

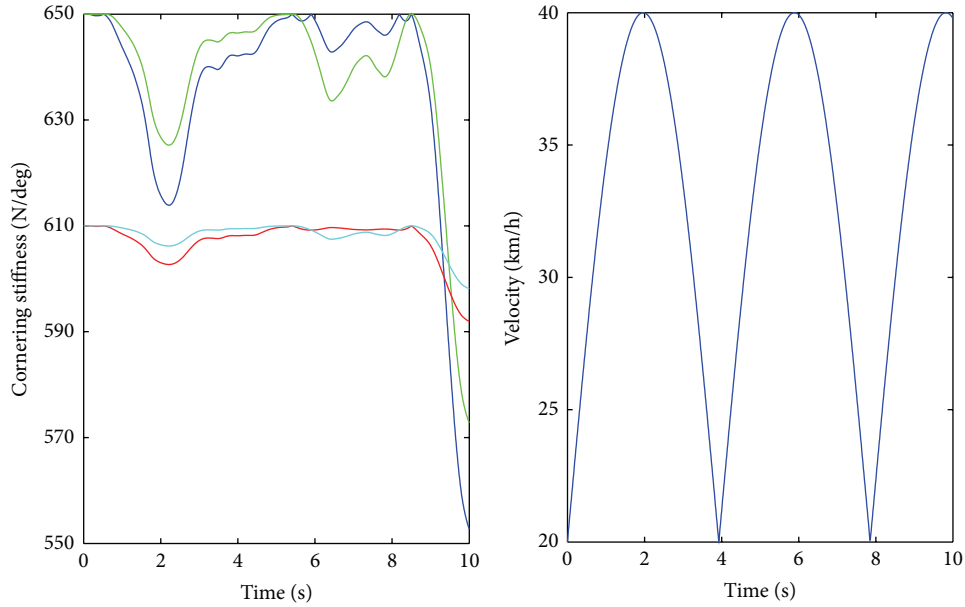

FIGURE 5: The uncertain parameters $C_{r_r}, C_{r_l}, C_{f_r}, C_{f_l}$ (blue, green, cyan, and red lines, resp.), and v.

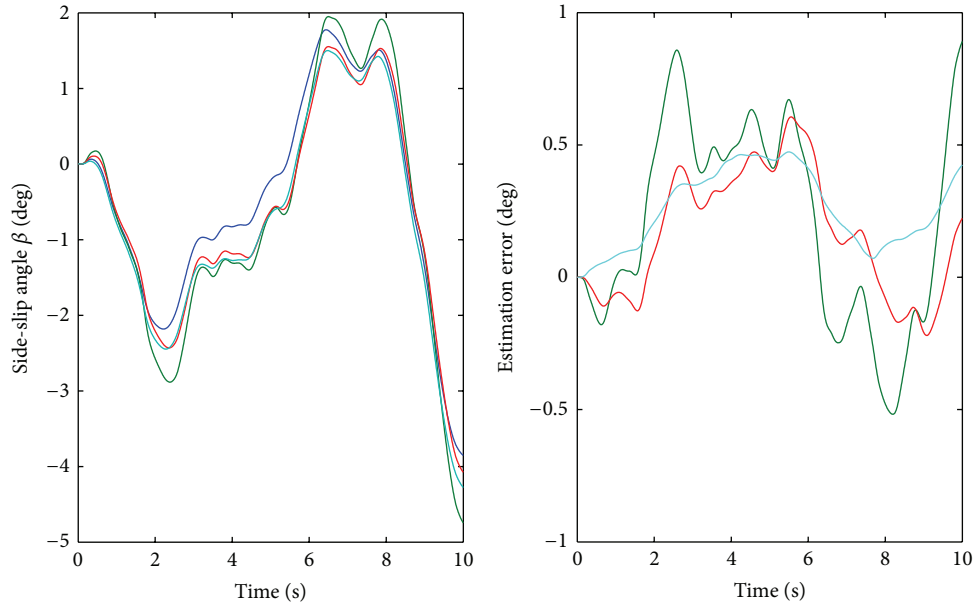

FIGURE 6: Side-slip angle (blue line) and the estimation results of the full-order estimator (cyan line) and first (green line) and second (red line) estimators.

changing the location of the central polynomial. The conservatism of the proposed technique is extremely dependent on the location of the central polynomial. For our example, we may use -0.2 and -0.1 instead of slow complex conjugate zeros $(-0.1 \pm i0.01)$ of central polynomial. In the sequel, we can obtain the second estimator as

$$\frac{y(s)}{x(s)} = \frac{3.1823s - 13.0733}{13.7075s + 1.6689}, \tag{33}$$

solving LMI problem with $c(s) = s^6 + 9.4278s^5 + 44.4695s^4 + 22.9787s^3 + 7.1576s^2 + 1.1772s + 0.0648$ central polynomial and ensuring $\gamma = 3.7817$. One can see the improvement on the dynamic response of the second estimator in Figure 6.

In the second part of the simulations, the nonlinear vehicle model is driven on the standard lateral dynamics maneuvers: sine with dwell and fish hook. In the design section, we consider the cornering stiffness parameters as uncertain in the limited interval. However, instantaneous cornering stiffness approaches to very low values when the lateral tyre forces are near their saturation. Experimental research shows that the lateral tyre forces are close to saturation level when the slip angle exceeds three degrees boundary [39]. Although

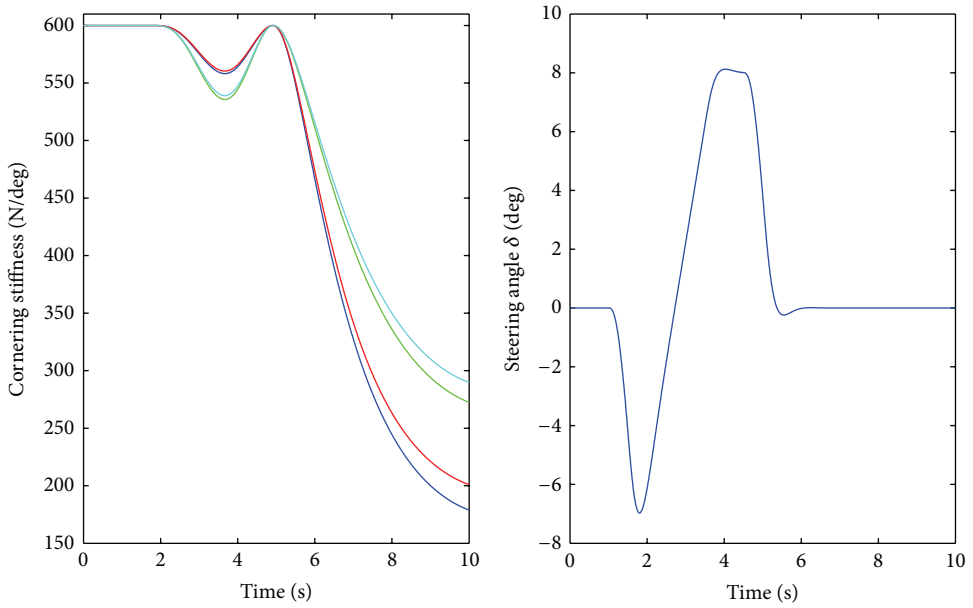

Figure 7: Cornering stiffness parameters $C_{r_r}, C_{r_l}, C_{f_r}, C_{f_l}$ (blue, green, cyan, and red lines, resp.) and the steer angle input for sine with dwell maneuver.

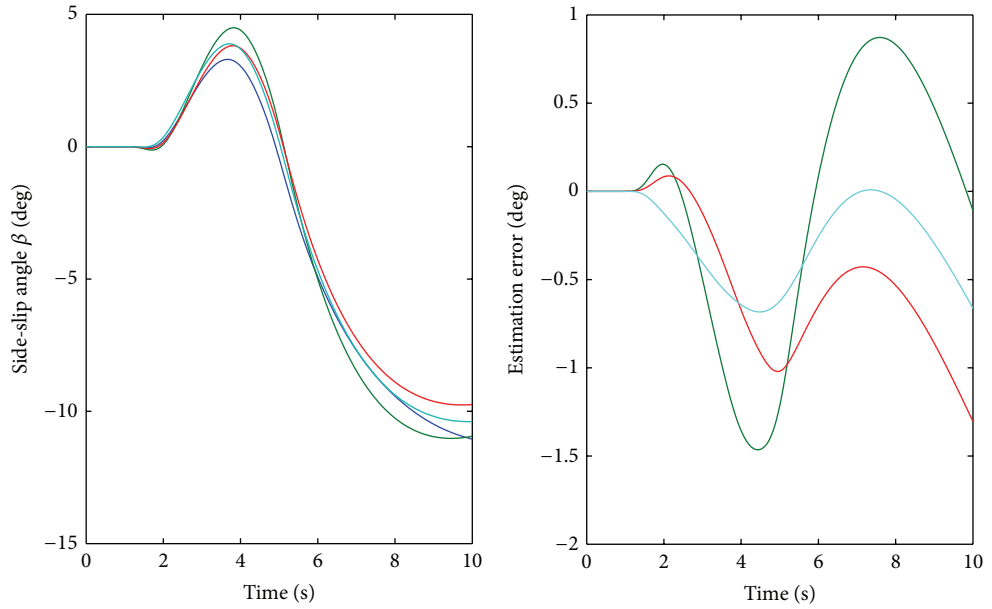

Figure 8: Side-slip angle (blue line) and the estimation results of the full-order estimator (cyan line) and first (green line) and second (red line) estimators.

the proposed estimators are designed with different intervals for cornering stiffness, their sensitivity level for parameter changes is low as an outgrowth fact of H_∞ optimization design. Here we compare the performance of our estimators with the full-order one and check the robustness against the parameter changes by using the sine with dwell maneuver. In order to make a realistic simulation, we constitute the cornering stiffness parameters for all four wheels by the help of Gaussian function. Figure 7 presents steer angle input and variation of cornering stiffness parameters. The results of sine with dwell maneuver under the same velocity profile used in the previous simulations are shown in Figure 8. During the sine and dwell maneuver, the cornering stiffness of tires exceeds our designed interval. Even in this case our second estimator presents very close performance to the full-order one. At the end of dwell part of maneuver, the vehicle body is slipping and loosing its lane. However, the stabilization is not the scope of this work.

Finally, the fish hook maneuver is used to check the performance of the proposed estimators at the extreme case.

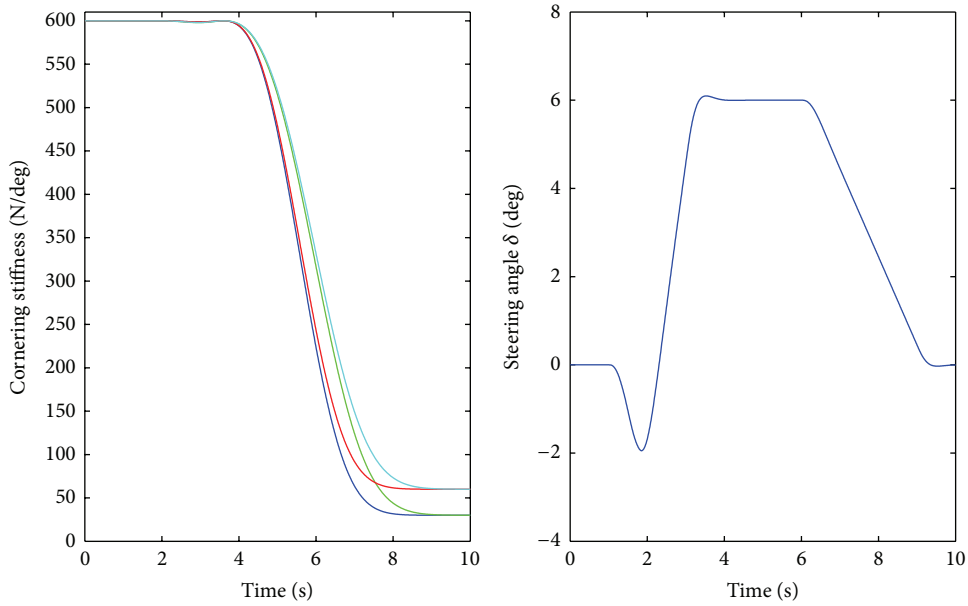

Figure 9: Cornering stiffness parameters C_{r_r}, C_{r_l}, C_{f_r}, C_{f_l} (blue, green, cyan, and red lines, resp.) and the steer angle input for fish hook maneuver.

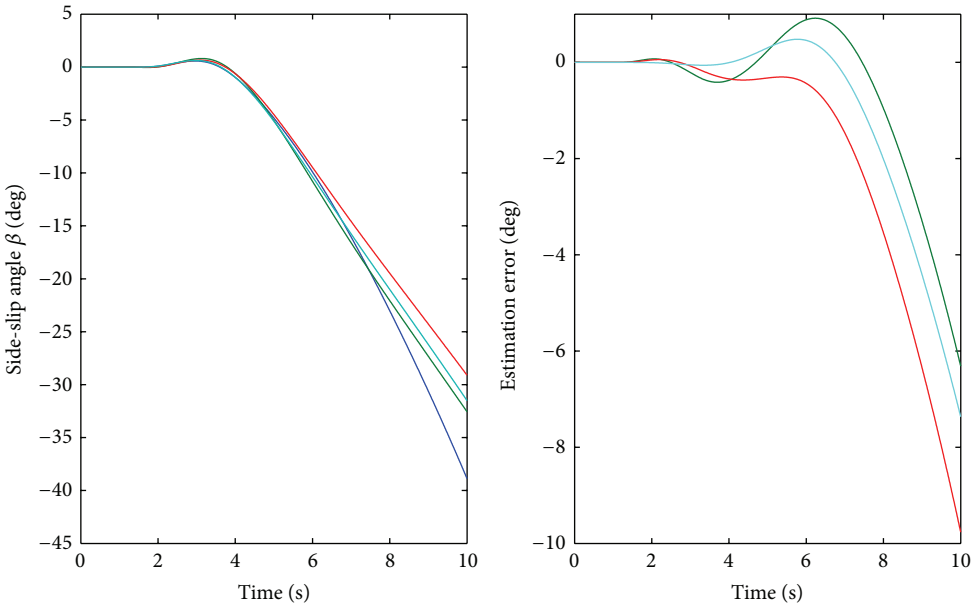

Figure 10: Side-slip angle (blue line) and the estimation results of the full-order estimator (cyan line) and first (green line) and second (red line) estimators.

In this example, we used constant velocity (30 km/h). One can obtain from the results shown in Figures 9 and 10 that the estimators provide favorable performance up to the extreme part of fish hook maneuver which starts at sixth second. While the estimators still follow the side-slip angle after the sixth second, the errors increase due to the drastic decrease of the cornering stiffness parameter. However, the skid prevention control or any control on lateral dynamics is not the scope of this work. One can conclude that the performance of the estimators at the extreme part of fish hook maneuver is at the satisfactory level.

6. Conclusion

In this paper, we revisit the classical side-slip angle estimation problem in the automotive industry. The presented method employs the positive realness to define a convex body in a nonconvex solution set in order to derive a low order estimator. Therefore, the technique provides suboptimal solution in terms of H_∞ norm of the transfer function between the steer angle and estimation error. In addition to this, the proposed technique can deal with uncertainties in a polytopic form, which are coming from the system parameters such

as cornering stiffness and velocity. Numerical simulations are used to validate the performance of the designed estimator. The results show that one can bound the H_∞ norm of proposed scheme via the first order estimator. Besides the disadvantages of full-order estimator, explained in the numerical results part, the engineers in automotive industry are familiar with low degree controllers and estimators such as PI, PD, or PID. They may easily constitute and tune them with a limited hardware. Therefore these types of estimators are still popular. To sum up, our method develops a robust fix-order observer design technique to estimate the side-slip angle using the measurement of yaw rate.

Although the velocity of vehicle can be easily measured, our design procedure takes it as an uncertain parameter due to the inherent limitation of the proposed technique. However, the simulation shows that the variation of velocity plays an important role in the estimation of side-slip angle. As a future work, we plan to extend the design to adapt quasi-LPV systems. This extension would enable us to use a nonlinear model in the design procedure which would be more realistic and would increase the accuracy of the estimation.

Conflict of Interests

The author declares that there is no conflict of interests regarding the publication of this paper.

References

[1] A. T. van Zanten, "Bosch ESP systems: 5 years of experience," *SAE Technical Papers*, vol. 109, no. 7, pp. 428–436, 2000.

[2] H. E. Tseng, B. Ashrafi, D. Madau, T. A. Brown, and D. Recker, "The development of vehicle stability control at Ford," *IEEE/ASME Transactions on Mechatronics*, vol. 4, no. 3, pp. 223–234, 1999.

[3] R. Rajamani, *Vehicle Dynamics and Control*, Springer, Berlin, Germany, 2005.

[4] J. Ackermann and P. Blue, *Robust Control: The Parameter Space Approach*, Springer, 2002.

[5] G. Phanomchoeng, R. Rajamani, and D. Piyabongkarn, "Nonlinear observer for bounded Jacobian systems, with applications to automotive slip angle estimation," *IEEE Transactions on Automatic Control*, vol. 56, no. 5, pp. 1163–1170, 2011.

[6] H. E. Tseng, "A sliding mode lateral velocity observer," in *Proceeding of the 6th International Symposium on Advanced Vehicle Control (AVEC '02)*, pp. 387–392, Hiroshima, Japan, September 2002.

[7] V. Cerone, D. Piga, and D. Regruto, "Set-membership LPV model identification of vehicle lateral dynamics," *Automatica*, vol. 47, no. 8, pp. 1794–1793, 2011.

[8] A. Von Vietinghoff, M. Hiemer, and U. Kiencke, "Nonlinear observer design for lateral vehicle dynamics," in *Proceedings of the 16th Triennial World Congress of International Federation of Automatic Control (IFAC '05)*, pp. 988–993, July 2005.

[9] P. J. T. Venhovens and K. Naab, "Vehicle dynamics estimation using Kalman filters," *Vehicle System Dynamics*, vol. 32, no. 2-3, pp. 171–184, 1999.

[10] U. Kiencke and A. Daiß, "Observation of lateral vehicle dynamics," *Control Engineering Practice*, vol. 5, no. 8, pp. 1145–1150, 1997.

[11] H. F. Grip, L. Imsland, T. I. Fossen, T. A. Johansen, J. C. Kalkkuhl, and A. Suissa, "Nonlinear vehicle velocity observer with road-tire friction adaptation," in *Proceedings of the 45th IEEE Conference on Decision and Control (CDC '06)*, pp. 3603–3608, December 2006.

[12] M. Abe, Y. Kano, K. Suzuki, Y. Shibahata, and Y. Furukawa, "Side-slip control to stabilize vehicle lateral motion by direct yaw moment," *JSAE Review*, vol. 22, no. 4, pp. 413–419, 2001.

[13] F. Cheli, E. Sabbioni, M. Pesce, and S. Melzi, "A methodology for vehicle sideslip angle identification: comparison with experimental data," *Vehicle System Dynamics*, vol. 45, no. 6, pp. 549–563, 2007.

[14] H. F. Grip, L. Imsland, T. A. Johansen, T. I. Fossen, J. C. Kalkkuhl, and A. Suissa, "Nonlinear vehicle side-slip estimation with friction adaptation," *Automatica*, vol. 44, no. 3, pp. 611–622, 2008.

[15] S.-H. You, J.-O. Hahn, and H. Lee, "New adaptive approaches to real-time estimation of vehicle sideslip angle," *Control Engineering Practice*, vol. 17, no. 12, pp. 1367–1379, 2009.

[16] K. Nam, S. Oh, H. Fujimoto, and Y. Hori, "Estimation of sideslip and roll angles of electric vehicles using lateral tire force sensors through RLS and kalman filter approaches," *IEEE Transactions on Industrial Electronics*, vol. 60, no. 3, pp. 988–1000, 2013.

[17] M. C. Best, T. J. Gordon, and P. J. Dixon, "Extended adaptive Kalman filter for real-time state estimation of vehicle handling dynamics," *Vehicle System Dynamics*, vol. 34, no. 1, pp. 57–75, 2000.

[18] L. Xie and C. E. de Souza, "Robust filtering for linear systems with parameter uncertainty," in *Proceedings of the 34th IEEE Conference on Decision and Control*, vol. 2, pp. 2087–2092, IEEE, December 1995.

[19] T. H. Lee, W. S. Ra, T. S. Yoon, J. B. Park, S. Y. Jung, and J. E. Seo, "Robust filtering for linear discrete-time systems with parametric uncertainties: a krein space estimation approach," in *Proceedings of the 42nd IEEE Conference on Decision and Control*, vol. 2, pp. 1285–1290, December 2003.

[20] J. C. Geromel, "Optimal linear filtering under parameter uncertainty," *IEEE Transactions on Signal Processing*, vol. 47, no. 1, pp. 168–175, 1999.

[21] R. M. Palhares and P. L. Peres, "Robust $\mathscr{H}_\infty$-filtering design with pole placement constraint via linear matrix inequalities," *Journal of Optimization Theory and Applications*, vol. 102, no. 2, pp. 239–261, 1999.

[22] A. Wu and G. Duan, "Robust H-infinity estimation for continuous-time polytopic uncertain systems," *Journal of Control Theory and Applications*, vol. 3, no. 4, pp. 393–398, 2005.

[23] K. Zhou, J. C. Doyle, K. Glover et al., *Robust and Optimal Control*, vol. 40, Prentice Hall, Englewood Cliffs, NJ, USA, 1996.

[24] D. Henrion, M. Sebek, and V. Kucera, "Positive polynomials and robust stabilization with fixed-order controllers," *IEEE Transactions on Automatic Control*, vol. 48, no. 7, pp. 1178–1186, 2003.

[25] A. Neumaier, "Complete search in continuous global optimization and constraint satisfaction," *Acta Numerica*, vol. 13, no. 1, pp. 271–369, 2004.

[26] D. Henrion and J.-B. Lasserre, "Solving nonconvex optimization problems," *IEEE Control Systems*, vol. 24, no. 3, pp. 72–83, 2004.

[27] D. Henrion, "LMI optimization for fixed-order H_∞ controller design," in *Proceedings of the IEEE Conference on Decision and Control*, pp. 4646–4651, December 2003.

[28] F. Yang, M. Gani, and D. Henrion, "Fixed-order robust H_∞ controller design with regional pole assignment," *IEEE Transactions on Automatic Control*, vol. 52, no. 10, pp. 1959–1963, 2007.

[29] A. G. Ulsoy, H. Peng, and M. Çakmakci, *Automotive Control Systems*, Cambridge University Press, Cambridge, Mass, USA, 2012.

[30] D. Henrion, D. Arzelier, and D. Peaucelle, "Positive polynomial matrices and improved LMI robustness conditions," *Automatica*, vol. 39, no. 8, pp. 1479–1485, 2003.

[31] W. Gilbert, D. Henrion Didier, J. Bernussou, and D. Boyer, "Polynomial LPV synthesis applied to turbofan engines," *Control Engineering Practice*, vol. 18, no. 9, pp. 1077–1083, 2010.

[32] M. C. de Oliveira and R. E. Skelton, "Stability tests for constrained linear systems," in *Perspectives in Robust Control*, pp. 241–257, Springer, 2001.

[33] V. Kučera, "Diophantine equations in control—a survey," *Automatica*, vol. 29, no. 6, pp. 1361–1375, 1993.

[34] H. Kwakernaak, "Robust control and H_∞-optimization—tutorial paper," *Automatica*, vol. 29, no. 2, pp. 255–273, 1993.

[35] U. Kiencke and L. Nielsen, *Automotive Control Systems: For Engine, Driveline, and Vehicle*, Springer, New York, NY, USA, 2005.

[36] J. C. Doyle, K. Glover, P. P. Khargonekar, and B. A. Francis, "State-space solutions to standard H_2 and H_∞ control problems," *IEEE Transactions on Automatic Control*, vol. 34, no. 8, pp. 831–847, 1989.

[37] J. Löfberg, "YALMIP: a toolbox for modeling and optimization in MATLAB," in *Proceedings of the IEEE International Symposium on Computer Aided Control System Design*, pp. 284–289, September 2004.

[38] J. F. Sturm, "Using SeDuMi 1.02, A Matlab toolbox for optimization over symmetric cones," *Optimization Methods and Software*, vol. 11, no. 1–4, pp. 625–653, 1999.

[39] U. Grundström and M. Nano, *Analysis of vehicle behavior to find criteria for steering robot tests [M.S. thesis]*, Luleå University of Technology, 2011.